Increasing the Diversity and Understanding of Semiconductor Nanoplatelets by Colloidal Atomic Layer Deposition

*Annett Reichhelm, René Hübner, Christine Damm, Kornelius Nielsch,
and Alexander Eychmüller**

Nanoplatelets (NPLs) are a remarkable class of quantum confined materials with size-dependent optical properties, which are determined by the defined thickness of the crystalline platelets. To increase the variety of species, the colloidal atomic layer deposition method is used for the preparation of increasingly thicker CdSe NPLs. By growing further crystalline layers onto the surfaces of 4 and 5 monolayers (MLs) thick NPLs, species from 6 to 13 MLs are achieved. While increasing the thickness, the heavy-hole absorption peak shifts from 513 to 652 nm, leading to a variety of NPLs for applications and further investigations. The thickness and number of MLs of the platelet species are determined by high-resolution transmission electron microscopy (HRTEM) measurements, allowing the interpretation of several contradictions present in the NPL literature. In recent years, different assumptions are published, leading to a lack of clarity in the fundamentals of this field. Regarding the ongoing scientific interest in NPLs, there is a certain need for clarification, which is provided in this study.

Semiconductor nanoplatelets (NPLs) gained large scientific interest during the last years, combining the remarkable size-dependent properties of nanomaterials with the precision of molecular substances. In small particles with extensions in the order of the de Broglie wavelength of the electron, quantum confinement leads to a strong influence of the particle size on the material properties, determining the bandgap and the positions of absorption and emission peaks. In contrast to nanoparticles, which always show a size distribution and peak broadening, NPLs of one species are reported to possess one defined thickness, leading to a defined electronical structure and narrow emission peaks.[1,2] These properties are highly requested for the application of nanomaterials, enabling the advancement of field-effect transistors,[3] phototransistors,[4] lasers,[5,6] sensors,[7] and solar concentrators.[8]

NPLs were first synthesized in 2008 by Ouyang et al., but were mistaken for magic-sized clusters[9] until Ithurria and Dubertret identified the material as few-nanometers-thick platelets, showing 1D quantum confinement along the thickness dimension and remarkable optoelectronic features.[1] In consequence, the field of NPL research emerged, yielding numerous findings and materials.

Until 2018, CdSe NPLs with thicknesses between two and five monolayers (MLs) were known, the latter consisting of five CdSe crystal layers and one additional terminating layer of cadmium ions.[10] The lack of success in the preparation of thicker NPLs raised many questions about the formation mechanism and limited the amount of available NPL species for research and application. The observed impossibility to produce thicker NPLs has been explained by Riedinger et al. with energy differences of the growth of different facets.[10]

In 2018, two different methods for the synthesis of thicker CdSe NPLs were shown by Chu et al.,[11] Christodoulou et al.,[12] and Cho et al.[13] Chu and co-workers used a colloidal atomic layer deposition (c-ALD) method published by Ithurria and Talapin,[14] whereas the two latter publications reported halide-supported syntheses, leading to thicker NPL species.[12,13]

In this study, we used a modification of the c-ALD method used by Chu et al.[11] to prepare a large variety of CdSe NPL species for optoelectronic investigations. While gas phase deposition techniques, such as atomic layer epitaxy (ALE)[15] and atomic layer deposition (ALD),[16] enable the preparation of defined films on flat substrates, c-ALD allows the epitaxial growth of additional crystal layers at the surface of dispersed nanoparticles. The idea behind this approach is the stepwise increase in the NPL thickness by the alternating adsorption of layers of cadmium and

A. Reichhelm, Prof. A. Eychmüller
Physical Chemistry
Technische Universität Dresden
Bergstraße 66b, 01069 Dresden, Germany
E-mail: alexander.eychmueller@chemie.tu-dresden.de

Dr. R. Hübner
Helmholtz-Zentrum Dresden-Rossendorf
Bautzner Landstraße 400, 01328 Dresden, Germany

C. Damm, Prof. K. Nielsch
Leibniz-Institut für Festkörper- und Werkstoffforschung Dresden
Helmholtzstraße 20, 01069 Dresden, Germany

selenide ions on the surfaces of the NPLs (for details, please see Experimental Section).

Surprisingly, there is a discrepancy in the literature concerning the described growth mechanism, leading to different concepts of the thickness of the prepared NPLs. While Ithurria and Talapin describe an "addition of one CdS monolayer on both sides" of an NPL, which corresponds to a gain of two monolayers per shelling step,[14] Chu et al. assume that "at each step, the NPL thickness increases by half a lattice parameter,"[11] which is only one ML. The latter assumption became the basis for the classification of thicker NPLs,[12,13] although the simultaneous absorption of selenide ions on both terminating cadmium facets seems to be more plausible due to the identical conditions on both sides of the platelet.

Because the thickness is crucial for the application and the understanding of the optoelectronical properties of each NPL species, there is a certain need for clarification, which we intend to answer in this study. Therefore, we prepared and examined a series of CdSe NPL species reaching from 4 to 13 MLs and shifting the characteristic heavy-hole (HH) absorption peak from 513 to 652 nm. The thickness increase was examined by absorption spectroscopy and high-resolution transmission electron microscopy (HRTEM), giving evidence for a two-monolayer increase in the thickness and disprove several common misconceptions of the NPL thickness in the scientific literature, increasing the general understanding of NPLs.

In the literature, NPLs are classified by the ML number as a measure for the thickness of the crystalline platelet. One CdSe ML consists of one layer of cadmium ions and one selenide layer. Because these NPLs are terminated by cadmium on both sides, there is an additional Cd^{2+} layer on the top side of every platelet (**Figure 1**). Surprisingly, there are still differences in the designation of the NPL species, leading to inconsistencies and misapprehensions, which we aim to resolve in the following section.

Due to the successive decrease in the electron density of the electron shell, there is no distinct boundary of an atom or atomic layer. Accordingly, considering the extension of a crystal, the most distinct description is the distance between the centers of the terminating atomic layers. The thickness of a two-monolayer NPL equals one CdSe unit cell with a lattice constant of 0.608 nm,[1] reaching from the center of the cadmium ions of the first monolayer to the center of the additional cadmium plane on top of the second monolayer. A four-monolayer thick (4-ML) NPL consists of four alternating layers of cadmium and selenide ions and one additional cadmium layer. Hence, the thickness equals two CdSe unit cells, which is 1.216 nm.
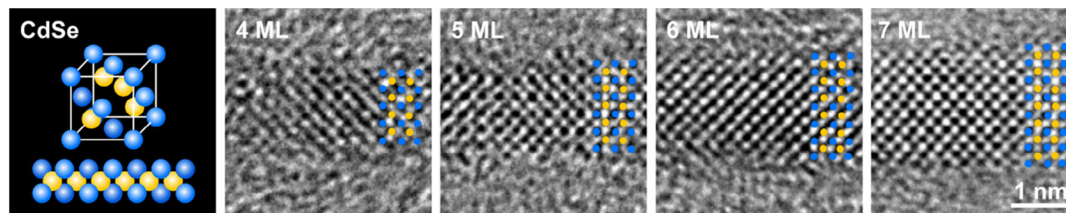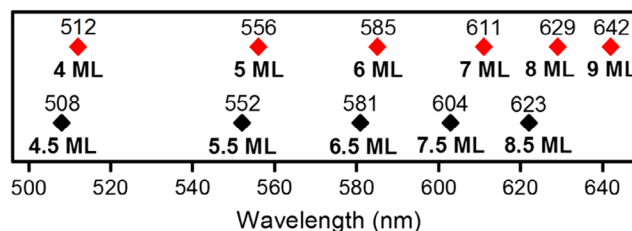
Figure 2. Differences in the peak positions and ML numbers of the CdSe NPL species reported by Chu et al.[11] (red) and Christodoulou et al.[12] (black) reveal a lack of clarity in the literature.

Because both facets of the NPL are terminated by cadmium ions, in some of the publications, NPL species are labeled with fractional numbers such as 4.5-ML.[12,17] While the aim of this approach is to stress the existence of the additional terminating cadmium layer, it hinders the calculation of the thickness. Calculating the thickness while adding half an ML leads to a larger value. This result could be considered as including the radii of the outer atomic layers, but in this context, adding half of an ML would be rather arbitrary, and we want to encourage the use of the integer numbers instead.

To date, NPLs of up to 9 MLs have been reported in the literature,[11,12] but the results are quite different (**Figure 2**). Even if the usual variation[1,18] in the reported peak wavelengths is considered, the differences appear to be too large to assign the NPLs to the same species. For example, Chu et al. reported 7-ML NPLs with an HH absorption peak at 611 nm,[11] whereas the 7-ML NPLs of Christodoulou et al. show this peak at 603 nm.[12] Additional unclarity is induced by Chu et al. using the c-ALD method of Ithurria and Talapin,[14] but using a different way of counting the added MLs. In the original publication, c-ALD is used to add alternating layers of sulfide and selenide to both faces of the CdSe NPLs, forming a shell of CdS, which is clearly shown by HRTEM.[14] Differing from this, Chu et al. assume the formation of new crystal layers at only one of the facets, leading to the increase in the NPL thickness by only one ML per shelling step.[11] Considering these observations, the labeling of these NPLs as 4- to 9-ML[11] has to be reconsidered.

To identify the NPL species, we used the c-ALD method[11,14] to samples of 4- and 5-ML NPLs. While the addition of one single monolayer to 4-ML NPLs should lead to a peak position typical for 5-ML NPLs after one shelling step, an increase in the thickness by two monolayers per step would lead to a larger value. Following these considerations, the shelling mechanism can be derived from experimental results. As shown in

Figure 1. Crystal structure of CdSe NPLs. Left: unit cell of zinc-blende cadmium selenide and schematic illustration of 1-ML CdSe with one terminating Cd^{2+} layer. Right: HRTEM of 4- to 7-ML NPLs revealing the successive increase in the thickness from 1.24 nm (4-ML) to 1.81 nm (6-ML) and from 1.53 (5-ML) to 2.09 nm (7-ML).
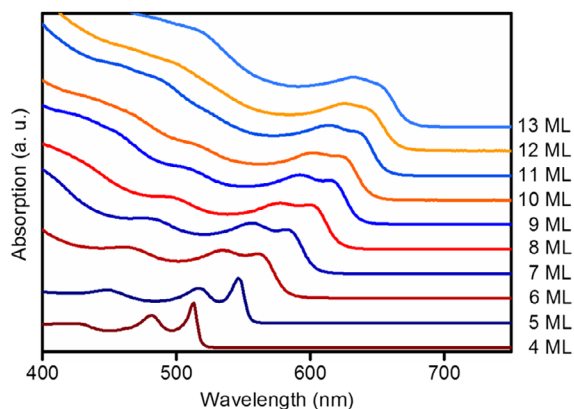
Figure 3. Absorption spectra of a series of CdSe NPLs prepared by c-ALD. The use of 4- and 5-ML NPLs as initial core material leads to the formation of even- (red) and odd-numbered (blue) NPLs via the addition of two monolayers per shelling step.

Figure 3, during one shelling step, the HH absorption peak shifts from 513 nm (4-ML) to 561 nm, which is significantly larger than the value of 546 nm of the 5-ML NPLs. Applying one shelling step to 5-ML NPLs leads to a further increase in the peak wavelength to 582 nm. These observations confirm the idea of the simultaneous adsorption of two monolayers of CdSe, challenging the labeling of the NPL species by Chu et al.[11]

To validate these findings, the synthesized 6- and 7-ML NPLs were examined by HRTEM and compared with the basic 4- and 5-ML NPLs, confirming a stepwise increase in the thickness and ML number (Figure 1). The theoretical thickness of the NPLs was calculated as the product of the ML number and the half lattice constant (0.304 nm[1]) of the CdSe unit cell. In the HRTEM images, the platelet thickness was measured accordingly as the distance of the centers of the outer planes of cadmium ions, yielding 1.24 nm (4-ML), 1.53 nm (5-ML), 1.81 nm (6-ML), and 2.09 nm (7-ML), which are in good agreement with the theoretical values (**Table 1**). These results reveal the existence of the 6-ML NPL species with a peak position

Table 1. Overview of the CdSe NPL species and the corresponding absorption peaks. The theoretical thickness was calculated as the product of the ML number and the half of the lattice constant (0.304 nm) of the CdSe unit cell.

ML number	Light hole (LH) peak [nm]	HH peak [nm]	Thickness [nm]
4	481	513	1.22
5	517	546	1.52
6	535	561	1.82
7	556	582	2.13
8	578	600	2.43
9	592	614	2.74
10	603	620	3.04
11	614	634	3.34
12	625	643	3.65
13	632	652	3.95

at 561 nm. The species with the peak at about 582 nm, which had been reported as 6-ML NPLs by Chu et al. (585 nm),[11] Christodoulou et al. (581 nm, 6.5-ML),[12] and Cho et al. (583 nm),[13] has been identified as 7-ML NPLs.

In the next step, the c-ALD method was applied to the previously prepared thicker NPLs, yielding an alternating series of increasingly thicker NPLs with even and odd ML numbers, based on 4- or 5-ML NPLs. In this study, a variety of CdSe NPL species with up to 13 MLs has been prepared (Table 1), shifting the HH absorption peak from 513 nm (4-ML) and 546 nm (5-ML) to 643 nm (12-ML) and 652 nm (13-ML). In the absorption spectra of these NPLs, the typical double peak is preserved while a gradual redshift can be observed due to the increase in the thickness (Figure 3 and Table 1). During the shelling process, the color of the NPL dispersion changes from yellow via red and green to brown, indicating the successful addition of further crystalline layers (**Figure 4**).

By comparing the measured peak positions to the literature, several similarities can be observed. However, there is a variation of the peak values between different publications and samples (Figure S1, Supporting Information). This observation challenges the idea of a series of accurate NPL species with identical optical features, which are exactly defined by the ML number, the material, and the crystal structure. While the reason for the differences is still not known, several parameters are assumed to influence the peak position of the NPL species, which are the small effect of the lateral dimensions[17,19] (in larger NPLs), the amount and type of the ligands, lattice defects, and local differences in the composition. Nevertheless, NPLs can be identified by the peak position. Most of the NPL species revealed in this study have been reported previously, but some of the ML labels have to be corrected.

Using a direct synthetic approach, Christodoulou et al.[12] were able to produce a variety of NPLs, but some species in between are missing. While the 508 and 552 nm NPLs (which are reported as 4.5- and 5.5-ML) are in good agreement with our 4- and 5-ML NPLs, the reported 6.5-, 7.5-, and 8.5-ML species at 581, 604, and 623 nm correlate with the 7-, 8-, and 10-ML NPLs observed in this study (Table 1).

Using the c-ALD method, Chu et al.[11] prepared a NPL sequence similar to this study, but only the 4-ML NPLs were used as starting material. Accordingly, by adding two monolayers in every shelling step, only even-numbered NPLs should have been prepared. Looking at the results (Figure 2), we find the usual 4-ML NPLs (512 nm), followed by species with the peaks at 556, 585, 611, 629, and 642 nm, which are reported as 5–9-ML but correlate with 5-, 7-, 9-, 11-, and 12-MLs, which show some disaccord with the assumption stated earlier. While the 5–11-ML species differ by two monolayers as predicted, the formation of 5-ML NPLs in the first step and 12-ML NPLs in the last step is in
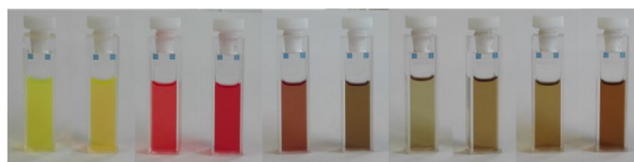

Figure 4. Color change of the CdSe NPL dispersions during the growth of additional crystal layers from yellow (4-ML) to brown (13-ML).

2000282 (3 of 5)

contradiction to the c-ALD theory[14] and to our observations. A possible explanation could be the formation of incomplete crystal layers. According to this idea, in the first step, starting with 4 MLs, 6-ML NPLs with incomplete outer layers were formed, decaying to 5-ML NPLs with an unusual high peak position at 556 nm. In the next steps, the growth of crystal layers proceeds as expected, leading to a series of unevenly numbered NPLs. When reaching 11 MLs, there is again an instability, leading to a value of 611 nm, which is quite low for 11-ML NPLs, and to the formation of 12- instead of 13-ML NPLs. During our study, such a dissolution of NPL layers has been observed when the reaction time and temperature were not high enough, offering a further possible explanation for the differences encountered in the NPL literature.

In addition to the identification of the NPL species reported in the literature, we observed two CdSe NPL species, which did not appear in the literature before, which are 6- and 13-ML NPLs with the peaks at 561 and 652 nm. The formation of even thicker NPLs via the c-ALD method leads to species, which can no longer be clearly identified by absorption spectroscopy due to the superposition of the peaks while approaching solid-state characteristics (Figure S1, Supporting Information).

To shine some light onto the growth mechanism, X-ray diffraction (XRD) measurements were conducted (**Figure 5**). For the initial 4- and 5-ML NPLs, a good agreement with literature data of the zinc-blende structure of cubic CdSe can be observed, as already shown by Ithurria et al.[20] After the addition of eight CdSe layers, the crystal structure remains unchanged, leading to very similar diffractograms and revealing an epitaxial growth of the additional lattice planes, as previously reported by Ithurria and Talapin for CdS shells.[14] The broadening of the reflections decreases with increasing thickness of the crystalline platelets due to the growing number of parallel lattice planes.[21]

While the increase in the thickness can be clearly observed by comparing the TEM images of the initial NPLs to the final 12- and 13-ML NPLs (**Figure 6**), the lateral extension stays the same during the shelling process. Accordingly, additional material is exclusively attached to the large facets, increasing the thickness. TEM images of all prepared NPL species is shown in the Supporting Information (Figure S2, Supporting Information).
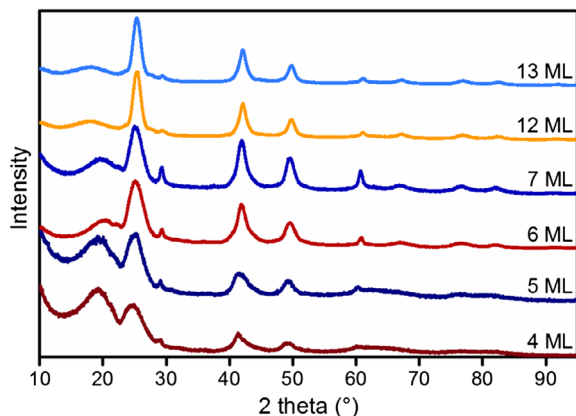

Figure 5. XRD measurements reveal the zinc-blende structure of the material and the epitaxial growth of the additional crystal layers.
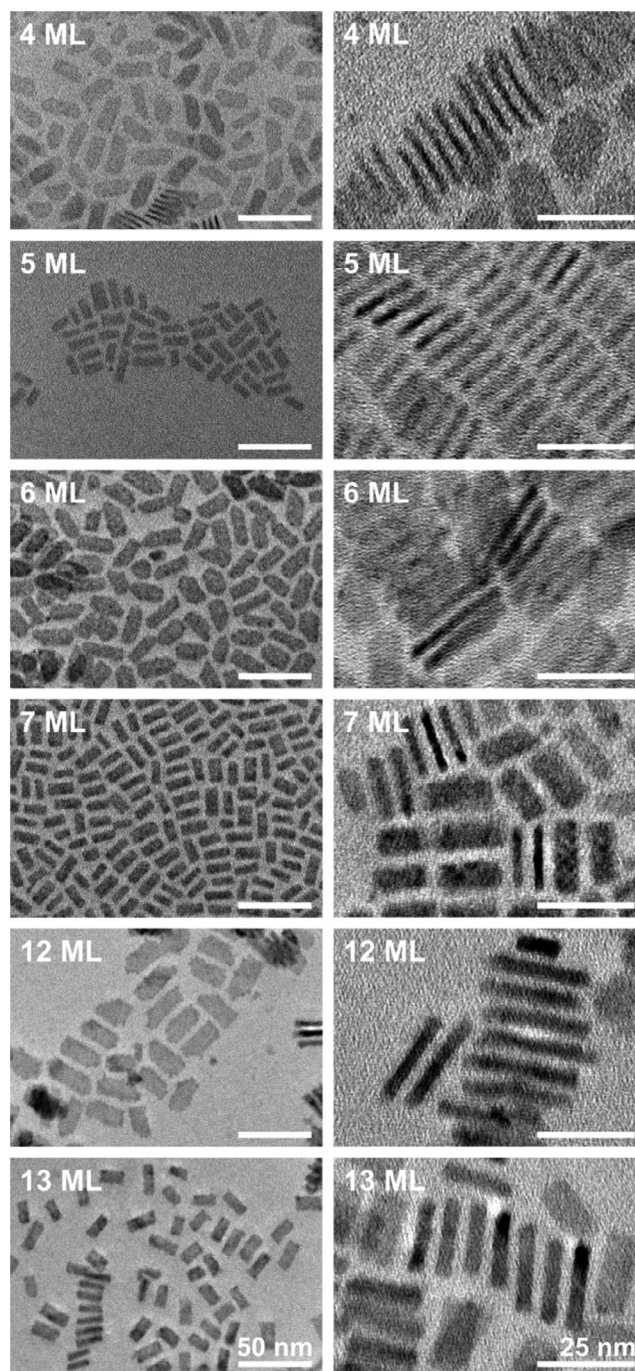

Figure 6. TEM images of CdSe NPLs of different ML numbers. Starting with 4- and 5-ML NPLs as core materials, a series of NPLs with up to 13 MLs were obtained.

In this article, we report the preparation and examination of a series of CdSe NPLs with increasing thickness, reaching from 4 to 13 MLs with HH absorption peaks between 513 and 652 nm. Therefore, alternating layers of cadmium and selenide ions were added using a c-ALD method,[11,14] leading to a variety of NPLs for optoelectronic investigations and application. In addition, we analyzed several contradictions in the NPL

literature, hopefully leading to an increase in clarity and understanding.

Experimental Section

CdSe NPL Synthesis: The initial NPLs were synthesized, following a slightly modified procedure published by Ithurria and Dubertret.[1]

For the synthesis of 4-ML NPLs, 70 mg of CdO (99.5%, Sigma-Aldrich), 340 mg of myristic acid (99%, Sigma-Aldrich), and 27 mL of octadecene (ODE; 90%, technical grade) were heated to 100 °C in a three-neck flask and were degassed under vacuum for 1 h. Subsequently, an argon flow was applied, and the temperature was increased to 285 °C, leading to the formation of cadmium myristate. After turning completely colorless, the solution was cooled to 105 °C using a water bath. After degassing for 30 min, a selenium suspension was added, which was prepared inside a glove box by mixing 24 mg of selenium mesh (ChemPur, 99.99%) and 3 mL of ODE followed by 30 min of sonication. After degassing for 30 min, argon was applied, and the reaction was heated to 240 °C. When reaching 200 °C, the solution turned dark yellow, and 160 mg of cadmium acetate dihydrate ($Cd(OAc)_2(H_2O)_2$, analytical grade) was added. At 240 °C, the reaction proceeded for 10 min and was than rapidly quenched to room temperature. Meanwhile, at 180 °C, 1 mL of oleic acid was added as ligand. The product was precipitated by the addition of 30 mL of hexane and 30 mL of ethanol followed by centrifugation, removing reactants and byproducts such as nanoparticles. The precipitate was dissolved in 4 mL of hexane and centrifuged to remove 3-ML NPLs.

For 5-ML NPLs, the procedure was the same, except for a few modifications. The myristate solution was formed at 300 °C and heated for about 15 min until turning to a turbid gray. The amount of $Cd(OAc)_2(H_2O)_2$ was increased to 240 mg, and for the NPL formation, the reaction was heated to 250 °C and proceeded for 10 min.

Layer-by-Layer CdSe Shell Growth: For the shell growth, a modified method was used based on the approach reported by Chu et al.[11] Under protection from oxygen, 24 mg of selenium mesh (ChemPur, 99.99%) suspended 1 mL of *N*-methylformamide (NMF; Alfa Aesar, 99%). Sodium borohydride (30 mg) ($NaBH_4$, Sigma Aldrich, 98%) was dissolved in 1 mL of NMF and 1 mL of ethanol. This solution was added slowly to the selenium suspension, leading to the reduction of the selenium to selenide under the formation of hydrogen. For the cadmium solution, 240 mg of cadmium acetate ($Cd(OAc)_2(H_2O)_2$, analytical grade) was dissolved in 2 mL of NMF. Concentrated NPL dispersion (200 μL) (with an extinction of 0.2 when 200 μL was diluted with 2 mL of hexane) was precipitated with ethanol and diluted in 2 mL of hexane. The addition of 2 mL of NMF led to the formation of a two-phase system, which had to be degassed to remove oxygen, which was required for the growth of the selenide layer. Afterward, 200 μL of the selenide solution was added followed by 5 min of vigorous shaking, leading to the phase transfer of the NPLs and a color change due to the additional selenide layers on both sides of each platelet. Then, the hexane phase was removed, and the NPLs were precipitated by the addition of 3 mL of toluene and 2 mL of acetonitrile followed by centrifugation. The precipitate was dispersed in 2 mL of hexane, and 250 μL of the cadmium solution was added. After shaking for 5 min, the reaction proceeded at 30 °C for 3 h. Afterward, 2 mL of hexane and 800 μL of oleic acid (Fisher Chemical, 70%) were added, and the NPLs were transferred to the organic phase by shaking. The NMF phase was removed, and the NPLs were precipitated by the addition of 2 mL of ethanol and centrifugation. The product was dispersed in 2 mL of hexane and could be used directly for the next shelling step.

Characterization: For absorption spectroscopy, a Cary 60 UV/Vis spectrophotometer from Agilent Technologies was used. Bright-field TEM images were obtained with a Tecnai G2 from FEI at 200 kV. HRTEM images were acquired with an image-C_s-corrected Titan 80–300 microscope from FEI operated at an accelerating voltage of 300 kV. For the XRD measurements, a D2 Phaser X-ray diffractometer of Bruker was used using the copper K_α line.

Supporting Information

Supporting Information is available from the Wiley Online Library or from the author.

Conflict of Interest

The authors declare no conflict of interest.

[1] S. Ithurria, B. Dubertret, *J. Am. Chem. Soc.* **2008**, *130*, 16504.
[2] J. Joo, J. S. Son, S. G. Kwon, J. H. Yu, T. Hyeon, *J. Am. Chem. Soc.* **2006**, *128*, 5632.
[3] E. Lhuillier, S. Pedetti, S. Ithurria, H. Heuclin, B. Nadal, A. Robin, G. Patriarche, N. Lequeux, B. Dubertret, *ACS Nano* **2014**, *8*, 3813.
[4] E. Lhuillier, A. Robin, S. Ithurria, H. Aubin, B. Dubertret, *Nano Lett.* **2014**, *14*, 2715.
[5] M. Li, M. Zhi, H. Zhu, W.-Y. Wu, Q.-H. Xu, M. H. Jhon, Y. Chan, *Nat. Commun.* **2015**, *6*, 1.
[6] C. She, I. Fedin, D. S. Dolzhnikov, P. D. Dahlberg, G. S. Engel, R. D. Schaller, D. V. Talapin, *ACS Nano* **2015**, *9*, 9475.
[7] G. K. Mani, J. B. B. Rayappan, *Sens. Actuators, B* **2014**, *198*, 125.
[8] A. H. Khan, V. Pinchetti, I. Tanghe, Z. Dang, B. Martín-García, Z. Hens, D. van Thourhout, P. Geiregat, S. Brovelli, I. Moreels, *Chem. Mater.* **2019**, *31*, 1450.
[9] J. Ouyang, M. B. Zaman, F. Y. Yan, D. Johnston, G. Li, X. Wu, D. Leek, C. I. Ratcliffe, J. A. Ripmeester, K. Yu, *J. Phys. Chem. C* **2008**, *112*, 13805.
[10] A. Riedinger, F. D. Ott, A. Mule, S. Mazzotti, P. N. Knüsel, S. J. P. Kress, F. Prins, S. C. Erwin, D. J. Norris, *Nat. Mater.* **2017**, *16*, 743.
[11] A. Chu, C. Livache, S. Ithurria, E. Lhuillier, *J. Appl. Phys.* **2018**, *123*, 035701.
[12] S. Christodoulou, J. I. Climente, J. Planelles, R. Brescia, M. Prato, B. Martín-García, A. H. Khan, I. Moreels, *Nano Lett.* **2018**, *18*, 6248.
[13] W. Cho, S. Kim, I. Coropceanu, V. Srivastava, B. T. Diroll, A. Hazarika, I. Fedin, G. Galli, R. D. Schaller, D. V. Talapin, *Chem. Mater.* **2018**, *30*, 6957.
[14] S. Ithurria, D. V. Talapin, *J. Am. Chem. Soc.* **2012**, *134*, 18585.
[15] R. B. Yang, N. Zakharov, O. Moutanabbir, K. Scheerschmidt, L.-M. Wu, U. Gösele, J. Bachmann, K. Nielsch, *J. Am. Chem. Soc.* **2010**, *132*, 7592.
[16] S. M. George, *Chem. Rev.* **2010**, *110*, 111.
[17] G. H. V. Bertrand, A. Polovitsyn, S. Christodoulou, A. H. Khan, I. Moreels, *Chem. Commun.* **2016**, *52*, 11975.
[18] D. Chen, Y. Gao, Y. Chen, Y. Ren, X. Peng, *Nano Lett.* **2015**, *15*, 4477.
[19] S. Bose, Z. Song, W. J. Fan, D. H. Zhang, *J. Appl. Phys.* **2016**, *119*, 143107.
[20] S. Ithurria, M. D. Tessier, B. Mahler, R. P. S. Lobo, B. Dubertret, A. L. Efros, *Nat. Mater.* **2011**, *10*, 936.
[21] P. Scherrer, *Nachr. Ges. Wiss. Göttingen, Math.-Phys. Kl.* **1918**, *2*, 98.